Available online at www.sciencedirect.com
SCIENCE DIRECT®
Bioorganic & Medicinal Chemistry 13 (2005) 661–669
Bioorganic & Medicinal Chemistry

Antileishmanial activity, cytotoxicity and QSAR analysis of synthetic dihydrobenzofuran lignans and related benzofurans

Sabine Van Miert,[a] Stefaan Van Dyck,[b] Thomas J. Schmidt,[c] Reto Brun,[d] Arnold Vlietinck,[a] Guy Lemière[b] and Luc Pieters[a,*]

[a]*Department of Pharmaceutical Sciences, University of Antwerp, Universiteitsplein 1, B-2610 Antwerp, Belgium*
[b]*Department of Chemistry, University of Antwerp, Groenenborgerlaan 171, B-2020 Antwerp, Belgium*
[c]*Institut für Pharmazeutische Biologie, Heinrich-Heine Universität Düsseldorf, Universitätsstrasse 1, D-40225 Düsseldorf, Germany*
[d]*Antiparasite Chemotherapy, Swiss Tropical Institute, Socinstrasse 57, CH-4002 Basel, Switzerland*

Received 17 May 2004; accepted 27 October 2004

Abstract—A series of synthetic dihydrobenzofuran lignans and related benzofurans were evaluated for their cytotoxicity in a screening panel consisting of various human tumour cell lines, and for their antiprotozoal activity against *L. donovani* (axenic amastigotes), chloroquine resistant *Plasmodium falciparum* (strain K1), *Trypanosoma brucei rhodesiense* and *T. cruzi*, and for cytotoxicity on L6 cells. No promising cytotoxicities against human tumour cell lines were observed for newly synthesised compounds, but the dimerisation product of some lipophylic esters of caffeic acid, such as compound **2g**, showed a high activity against chloroquine-resistant *P. falciparum* (strain K1) (IC_{50} 0.43 μg/mL) and *L. donovani* (axenic amastigotes) (IC_{50} 0.12 μg/mL), which was confirmed in an infected macrophage assay (IC_{50} 0.19 μg/mL). QSAR models for the cytotoxic and antileishmanial activity were generated using *Quasar* receptor surface modelling.

1. Introduction

Leishmaniasis is a tropical and subtropical disease occurring in three different clinical forms (cutaneous, muco-cutaneous and visceral), which is caused by protozoal parasites of the genus *Leishmania*. In very much the same way as for some other neglected diseases caused by protozoa such as malaria (*Plasmodium falciparum* and other *Plasmodium* sp.), African trypanosomiasis (sleeping sickness) (*Trypanosoma brucei rhodesiense* and *gambiense*) and American trypanosomiasis (Chagas' disease) (*Trypanosoma cruzi*), it remains a major public health problem in large areas of the world, because of the lack of effective and affordable drugs, or increasing resistance against existing drugs.[1] The identification of a suitable drug target is essential for effective drug development. Tubulin, a heterodimeric protein and the building block for microtubules, which play a crucial role in various cellular processes, including chromosome segregation during cell proliferation, is considered as a promising target for antiprotozoal chemotherapy.[2] The tubulins of humans and parasites have a different primary amino acid sequence and polymerisation properties, and it has been observed that traditional colchicine-site agents have little effect on protozoal tubulin.[3] Nevertheless leishmanicidal activity has been reported for analogues of combretastatin, which is a potent inhibitor of tubulin polymerisation, acting at the colchicine site.[4] Antileishmanial activity has also been reported for some lignans from *Virola* species and synthetic analogues; the highest activity was observed for some β-ketosulfides such as (3,4-dimethoxy)-8-(4′-methylthiophenoxy)-propiophenone. Preliminary mode of action studies suggested microtubule inhibition.[5] A series of synthetic dihydrobenzofuran lignans and related benzofurans, which contain the well-known pharmacophore for inhibitors of tubulin polymerisation binding at the colchicine site, that is, two variable aromatic domains kept in a non-planar arrangement by different linkers, also present in combretastatin derivatives and the β-ketosulfide analogues mentioned above, were found in our previous work to

Keywords: Dihydrobenzofuran lignans; *Leishmania*; Cytotoxicity; QSAR.
* Corresponding author. Tel./fax: +32 3 820 27 09; e-mail: luc.pieters@ua.ac.be

0968-0896/$ - see front matter © 2004 Elsevier Ltd. All rights reserved.
doi:10.1016/j.bmc.2004.10.058

display cytotoxic (against human tumour cell lines) and antitubulin properties.[6,7] Obviously different structure–activity relationships will apply for interactions with human and protozoal tubulin, and hence also for cytotoxicity on human cells and protozoa. Therefore it appeared appropriate to evaluate and to compare the antiprotozoal (antiplasmodial, antitrypanosomal and antileishmanial) and cytotoxic properties of a series of known and newly synthesised dihydrobenzofuran lignans and benzofuran derivatives, and to apply quantitative structure–activity relationship (QSAR) models based on *Quasar* receptor surface modelling. These investigations have led to the characterisation of the dihydrobenzofuran derivative **2g** as a promising antileishmanial lead compound.

2. Results and discussion

2.1. Cytotoxicity on human cancer cell lines

Evaluation of **2a–d**, **3a–d**, **4a–d**, **5d** and **6d** in an in vitro human disease oriented tumour cell line screening panel, consisting of 60 human tumour cell lines, at the National Cancer Institute (NCI, Bethesda, MD, USA) has been published before.[6] All other compounds reported here were tested in the same assay (see Supporting information). More particularly the sterically hindered esters **2f–i** were prepared because the corresponding methyl ester **2b** was found to have a pronounced cytotoxic activity, especially against the breast cancer cell lines MB-435, MDA-N and BT-549 where GI_{50} values <10 nM were observed (drug concentration, which reduces cell growth to 50% of level obtained with untreated cells). However, in the hollow fibre assay for preliminary in vivo testing, it was not sufficiently active for further in vivo evaluation.[6] Because hydrolysis of the methyl esters might explain the loss of activity in vivo, the esters **2f–i**, which are less sensitive for hydrolysis than the methyl ester **2b**, were prepared. Unfortunately, as illustrated for **2i** in Table 1, these bulky esters lost most of there in vitro cytotoxicity: Against the three breast cancer cell lines mentioned above, GI_{50} values in the micromolar instead of the nanomolar range were observed, and these esters were not selected for further evaluation. Similarly, none of the newly synthesised dihydrobenzofuran or benzofuran derivatives described in the present work exhibited a promising cytotoxicity in the human tumour cell line panel, as evidenced by some selected characteristic compounds (Table 1).

Table 1. Inhibition of in vitro tumour cell growth (GI_{50}, μM)

	2i	4e	5j	6j
Average GI_{50}[a]	4.4	72.4	11.2	18.6
HL-60 (TB)[b]	2.2	60.3	24.0	14.5
K-562	2.6	33.9	12.0	10.0
NCI-H522	1.7	70.8	9.8	1.9
HCT-15	4.2	75.9	15.5	11.7
SF-539	2.6	>100	1.5	21.4
M14	6.2	97.7	14.8	17.4
OVCAR-3	4.6	>100	17.4	20.4
UO-31	5.0	>100	15.1	20.4
DU-145	4.4	>100	9.1	21.9
MB-435	3.5	24.0	4.4	5.1
MDA-N	4.2	31.6	5.2	6.9
BT-549	13.2	>100	14.5	22.9

[a] Average log GI_{50} values calculated from all cell lines tested.

[b] HL-60 (TB), K-562, leukaemia cell lines; NCI-H522, non-small-cell lung cancer cell line; HCT-15, colon cancer cell line; SF-539, CNS cancer cell line; M14, melanoma cell line; OVCAR-3, ovarian cancer cell line; UO-31, renal cancer cell line; DU-145, prostate cancer cell line; MDA-MB-435, MDA-N, BT-549, breast cancer cell lines.

2.2. Antiprotozoal activity

Because of the antileishmanial activity reported before for some lignans containing two variable aromatic domains (see above), a series of our dihydrobenzofuran lignans and related benzofuran derivatives was evaluated against the protozoa *Leishmania donovani* (axenic amastigotes), chloroquine resistant *P. falciparum* (strain K1), *T.b. rhodesiense* and *T. cruzi*, and for cytotoxicity on L6 cells. Results are shown in Table 2 except for *T. cruzi* for which no promising activities were observed. Against *P. falciparum*, **2g** showed an IC_{50} of 0.43 μg/mL, and **5j** 1.06 μg/mL. Most interesting activities, however, were observed against *L. donovani*. In a prescreen against axenic amastigotes, three compounds showed an IC_{50} around or below 0.1 μg/mL (**2f**, **2g** and **2h**), and their activity was confirmed in an antileishmanial assay carried out in infected macrophages. In the latter assay, **2g** was the most active compound, showing an IC_{50} of 0.19 μg/mL. Remarkably, the lipophylic esters **2f**, **2g** and **2h** were prepared as analogues of the methyl-ester **2b**, which was the most promising inhibitor of tubulin polymerisation and the most cytotoxic compound against human tumour cell lines, as demonstrated in our previous investigations.[6] However, the antileishmanial activity of **2b** was almost two orders of magnitude lower than observed for **2f** or **2h**. Apparently in the dihydrobenzofuran series the introduction of larger ester group decreases the cytotoxicity, while enhancing the antileishmanial activity. Although also some benzofuran derivatives such as **5j**, **6d** or **6j** showed antileishmanial IC_{50} values <1 μg/mL, they did not show a pronounced activity in the assay in infected macrophages, and the dihydrobenzofuran derivatives were given priority for further evaluation. Compound **2g** was selected for in vivo evaluation, although the development of more active and less cytotoxic analogues may be necessary before a clinically useful compound will be obtained.

2.3. QSAR analysis

Since a better quantitative understanding of the structure–activity relationships underlying some of the compounds' selectivity with respect to cytotoxic or antiprotozoal activity would be a prerequisite for a rational application of structural changes in order to arrive at more selective antiprotozoal drug leads, a 4D-QSAR study using the concept of quasi-atomistic receptor surface modelling (*Quasar*) was carried out. For a detailed description of *Quasar* methodology see literature.[8,9] Based on the assumption that the compounds under study act specifically at a common target site

Table 2. Antileishmanial, antiplasmodial, antitrypanosomal and cytotoxic (L6 cells) activity (IC_{50}, μg/mL)

	Leishmania donovani (axenic amastigotes)	*Leishmania donovani* (infected macrophages)[a]	*Plasmodium falciparum* K1	*Trypanosoma brucei rhodesiense*	Cytotoxicity (L6 cells)
2b	1.9	—[b]	3.3	5.4	4.2
2c	2.7	—	3.2	18.2	5.2
2d	3.2	—	>5	27.8	—
2f	<0.04	2.6	3.3	5.5	7.4
2g	0.12	0.19	0.43 ± 0.01[c]	2.9	6.6
2h	<0.04	2.4	1.5	2.6	14.0
2j	0.6	dnp[d]	>5	14.3	12.1
3b	2.4	—	>5	8.0	7.5
4b	>30	—	>5	5.0	—
4d	>30	—	1.7	24.1	—
5d	2.3	—	>5	10.4	—
5j	0.7	>10	1.06 ± 0.18[b]	2.4	16.7
6d	0.3	6.3	1.6	>90	—
6j	0.6	>10	3.5	22.4	13.2
7d	6.2	—	4.5	3.8	—
7j	>30	—	>5	20.5	—
8j	19.9	—	>5	>90	—
9j	4.2	—	3.2	6.7	—
10j	>30	—	—	>90	—
Positive control[e]	0.25	0.12	0.065	0.0023	0.003

[a] Only antileishmanial activity of compounds showing an $IC_{50} < 1$ μg/mL in the assay on axenic amastigotes was confirmed in the assay on infected macrophages.
[b] —, not tested.
[c] Only compounds showing an antiplasmodial $IC_{50} < 1$ μg/mL were tested in duplicate (mean ± SD).
[d] dnp, determination not possible due to cytotoxicity on host cells.
[e] Positive controls used were: miltefosine for both leishmania assays, melarsoprol for *T.b. rhodesiense*, chloroquine for *P. falciparum* and podophyllotoxin for L-6 cells.

(presumably tubulin) in each cell system, binding site models were generated for the HL60-cytotoxic and the antileishmanial activity.

The model obtained for cytotoxic activity (*HL60*) is characterised by a squared correlation coefficient between experimental and predicted binding energy of $r^2 = 0.821$, a squared cross-validated correlation coefficient $q^2 = 0.808$ and a squared correlation coefficient for the test set prediction $p^2 = 0.715 \pm 0.099$. A plot of the predicted versus experimental binding energies for training and test set is shown in Figure 1 and the data are given in Table 3. The moderately high r^2 and q^2 values were caused by one compound of the training set, **10j**. Elimination of **10j** from the data set led to an increase of r^2 and q^2 to 0.917 and 0.900, respectively, but no improvement of the test set predictions was obtained (data not shown). The receptor envelope consists

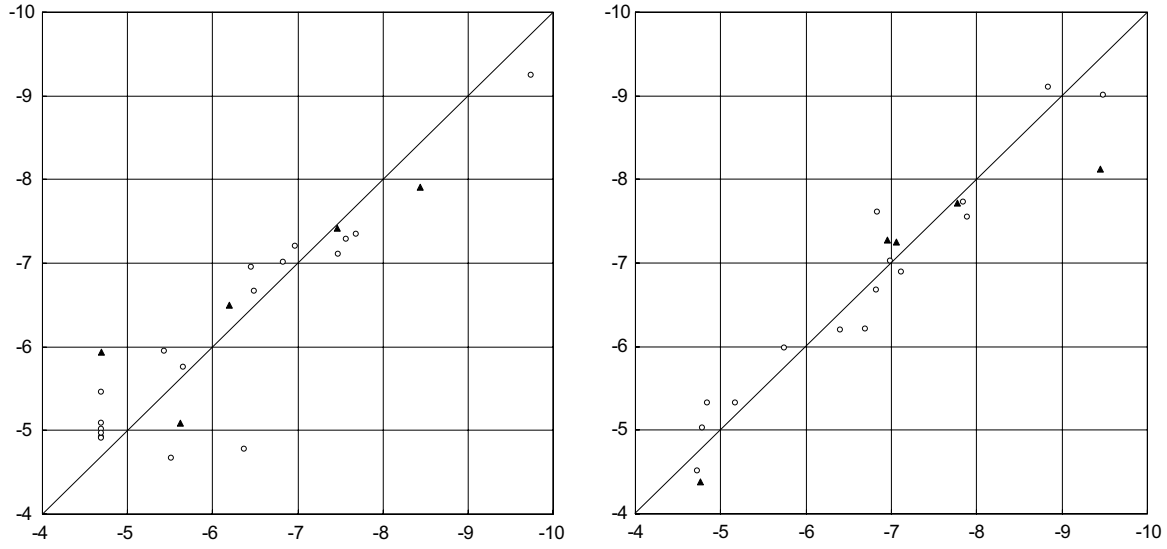

Figure 1. Predicted versus experimental binding energy (ΔG^0, kcal mol^{-1}) of neolignans in *Quasar* models. Left: cytotoxicity (*HL60*); right: Antileishmanial (*L. donovani*); circles: training set; triangles: test set.

Table 3. Experimental binding energies and values predicted by the Quasar models (ΔG^0_{293}, kcal mol^{-1})

	HL60		*LDON*	
	Exp.	Pred	Exp.	Pred
Training set				
2a	−6.972	−7.200		
2b	−9.747	−9.245	−7.116	−6.895
2d	−7.481	−7.109	−6.837	−7.608
2g			−8.839	−9.103
2h	−6.824	−7.011	−9.488	−9.007
2i	−7.575	−7.285		
2j			−7.885	−7.552
3a	−5.430	−5.950		
3b	−7.682	−7.349	−6.984	−7.023
3c	−6.449	−6.950		
4a	−5.510	−4.669		
4b	−4.692	−5.453	−4.721	−4.513
4c	−4.692	−4.971		
4d			−4.790	−5.027
4e	−5.658	−5.761		
6d	−4.692	−4.910	−6.820	−6.675
6j	−6.489	−6.670	−7.838	−7.733
7d			−6.406	−6.195
7j	−4.692	−4.926	−5.168	−5.325
8j	−4.692	−5.015	−5.745	−5.987
9j	−4.692	−5.085	−6.693	−6.212
10j	−6.368	−4.778	−4.849	−5.326
Test set				
2c	−8.433	−7.912	−6.953	−7.280
2f			−9.450	−8.125
3d	−7.468	−7.419		
4d	−5.617	−5.088		
5d	−4.692	−5.941	−7.063	−7.248
5j	−6.194	−6.499	−7.776	−7.722
9			−4.765	−4.386

of 257 virtual particles possessing mainly hydrophobic properties (76.7% = sum of VL0; hydrophobic neutral, VL5: hydrophobic positive and VL6: hydrophobic negative). The polar interactions are comprising particles interacting with electronegative structure elements of the ligand molecules (SB+ and Don: 18.9%) and such interacting with ligand parts possessing positive partial charge (SB- and Acc: 4.1%). One potential H-Bond flip-flop site (region where a structure element capable of both, H-bond donation and acceptance should be located) was identified. The induced fit scenario chosen during evolution of the model is related to energy minimisation along each compound's steric field vectors (envelope = fem). Multiple linear regression (MLR) of the individual contributions to the total predicted binding energy (van der Waals, electrostatic, hydrogen bonding, polarisation, solvation, entropy and induced fit energies) showed that the major part (88%) of the variance in $\Delta G^0_{(\mathrm{pred})}$ is explained by the electrostatic, H-bonding and induced fit terms. The regression equation obtained with these three terms was

$$-\Delta G^0_{(\mathrm{pred})} = -0.514E_{\mathrm{ele}} - 0.406E_{\mathrm{hbd}} - 5.883E_{\mathrm{IF}} + 0.721 \ (r^2 = 0.884),$$

indicating that more negative (i.e., favourable) electrostatic and H-bonding interactions as well as a lower induced fit energy (i.e., little energy required for shape adaptation of the binding site) lead to high activity (note that the equation uses the negative ΔG^0 since it is directly proportional to activity).

The model for antileishmanial activity (LDON) yielded $r^2 = 0.912$, $q^2 = 0.900$ and $p^2 = 0.782 \pm 0.067$. For a plot of predicted versus experimental binding energies (see Fig. 1). The p^2 value is excellent although the predicted value for the best compound (**2f**) is too low by more than 1 kcal mol^{-1} (factor ≈10 in IC_{50}). However, **2f** is still correctly predicted as the most potent compound in the test set. The binding site model consists of 287 virtual particles with similar overall properties as the HL60 model. On average, hydrophobic particles account for 83.4% of the total surface. Particles interacting with electronegative parts of the ligands constitute 11.8% and such interacting with electropositive parts 4.6%. As in the cytotoxicity model, one H-bond flip-flop site is present. The preferred induced fit mode in this case is related to adaptation of the individual compounds' envelopes to the mean envelope based on the molecular lipophilic potential (envelope = lip). MLR of the individual energy contributions (see above) identified the van der Waals-, electrostatic and solvation energy terms as most influential on the total predicted ΔG^0, which is explained to 82% by these factors. The regression equation obtained with these three terms was

$$-\Delta G^0_{(\mathrm{pred})} = -0.702E_{\mathrm{vdw}} - 1.351E_{\mathrm{ele}} + 0.337E_{\mathrm{solv}} + 1.227 \ (r^2 = 0.817),$$

showing that favourable van der Waals and electrostatic interactions associated with a less negative solvation energy (low penalty associated with desolvation, i.e., higher lipophilicity) lead to high activity.

As can be deduced from the relative distribution of properties on the receptor surface the model for LDON is slightly more hydrophobic than the cytotoxicity model HL60, which is due mainly to a decreased number of H-bond donor (Don, green) and salt-bridge-positive (SB+, red) particles in the former. In line with these observations, induced fit in LDON was modelled on the basis of the lipophilicity potential and van der Waals interactions with the receptor envelope as well as the energy penalty associated with desolvation were of higher importance than in HL60. Lipophilicity thus appears more influential on antileishmanial activity than on cytotoxicity. On the other hand, steric field related induced fit was used in HL60 and the induced fit energy term proved to be more influential in this model. Thus, the HL60 receptor appears to be more demanding with respect to the ligands' steric features. Considering the distribution of the different particle types on their surface, the binding sites are quite similar, that is, many points with identical or similar properties appear in corresponding positions. Most noteworthy, the mentioned H-bond flip-flop particle (violet) is found in an identical position on both surfaces (see Fig. 2). From this position, interactions with the pending phenyl ring's 4-OH and 4-OMe substituents are possible, most favourably in cases where this ring is in the 2β-position (i.e., 2R-configured non-planar compounds).

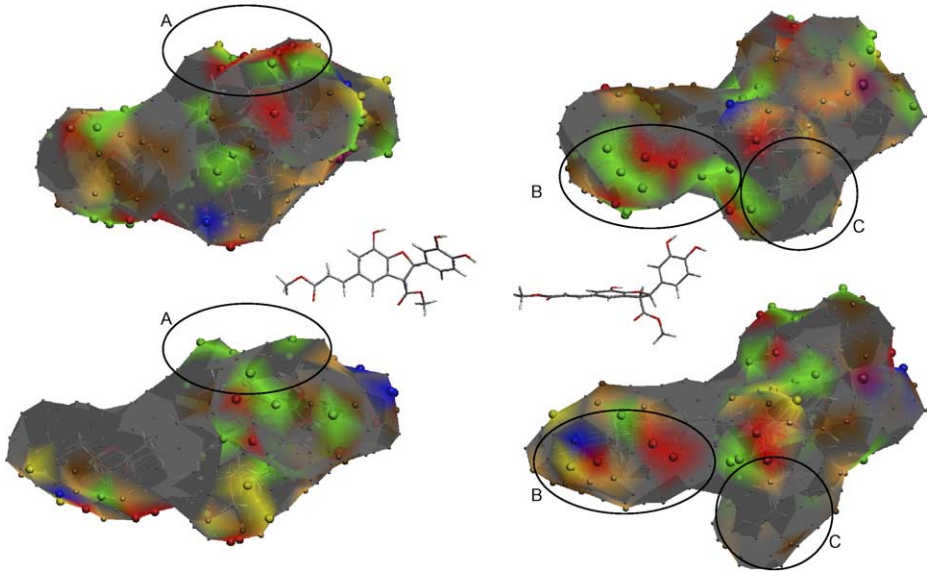

Figure 2. Receptor surface models for cytotoxic (top) and antileishmanial activity (bottom) with the aligned compounds under study, shown from two different viewing angles. The inset structures show compound **2b** in the respective relative orientation.

It becomes obvious from Figure 2 that there are two regions where particles engaged in polar (electrostatic and H-bonding) interactions concentrate. The first one lies on the 'top side' (left picture, region A), corresponding to interactions with the furan oxygen and the hydroxy- or methoxy groups at C-3′ of the benzofuran moiety. The second one is located on the 'lower side' around the ester groups at the C_3-side chain and at C-3 of the furan ring (right picture, region B). LDON shows less polar interactions in region A where it only possesses some H-bond donor particles indicating that this region is less important for antileishmanial activity. In region B, both models show mainly H-bond donating and SB+ particles interacting with the ester carbonyl groups. LDON additionally shows some H-bond acceptor (Acc, yellow) and a negative salt-bridge particle (SB−, blue), which can only interact favourably with the free alcoholic OH protons of some compounds (series **4** and **7**) or the acidic proton of **8j**. Their occurrence in the LDON model (the fact that they were not lost during model evolution) seems to indicate that such groups—irrespective of their tendency to render the compounds more hydrophilic causing a generally detrimental effect on activity—are somewhat better tolerated than in the HL60 binding site.

In order to interpret directly the impact of structural features on the differential activity observed with some compounds and to identify changes in substitution that might possibly lead to an increased selectivity towards LDON at lower cytotoxicity, molecular models of various untested compounds (structures **p1**–**p26**) were used as probes for the two binding site models by predicting their activity (e.g., see Table 4; a full list of these

Table 4. ΔG^0 values predicted in the HL60 and LDON receptor surface models for some non-existent probe molecules in comparison with **2a**, **2b** and **2g** illustrating the influence of the phenolic OH group at C-3 and of the ester groups at C-9′ and C-9 as major determinants of selective activity

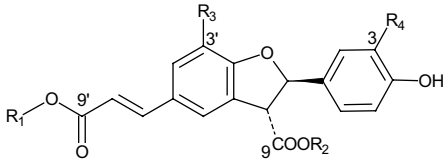

	R_1	R_2	R_3	R_4	$\Delta G^0_{pred(HL60)}$	$\Delta G^0_{pred(LDON)}$	$\delta\Delta G^0$	*rel* IC_{50}
2a	Me	Me	H	H	−7.200	−6.158	1.042	0.167
2b	Me	Me	OH	OH	−9.245	−6.895	2.350	0.018
p1	Me	Me	H	OH	−8.998	−6.561	2.436	0.015
p2	Me	Me	OH	H	−7.473	−6.716	0.757	0.276
p3	*n*Bu	*n*Bu	H	H	−7.376	−8.301	−0.925	4.926
2g	*n*Bu	*n*Bu	OH	OH	−8.077	−9.103	−1.026	5.952
p4	*n*Bu	*n*Bu	H	OH	−8.249	−8.940	−0.691	3.333
p5	*n*Bu	*n*Bu	OH	H	−7.183	−8.574	−1.391	10.980
p20	*n*Bu	Me	OH	H	−7.680	−7.791	−0.111	1.211
p21	Me	*n*Bu	OH	H	−6.529	−7.599	−1.070	6.289

$\delta\Delta G^0$: $\Delta G^0_{pred(LDON)} - \Delta G^0_{pred(HL60)}$; *rel* IC_{50}: ratio of predicted IC_{50} values (pred IC_{50} HL60)/(pred IC_{50} LDON); higher value corresponding to higher selectivity versus LDON.

structures and their predicted binding energies is available as Supporting information). Firstly, the influence of the phenolic substituents corresponding to region A was investigated by comparing the predictions for **2a** (3,3′-H) and **2b** (3,3′-OH) with the monophenols (**p1**: 3-OH, 3′-H and **p2**: 3-H, 3′-OH). It was observed that elimination of the phenolic OH at C-3′ in the benzofuran moiety does not lead to any dramatic changes in either the predicted HL60 or LDON activity. Contrastingly, replacement of the C-3 OH at the pending phenyl ring by a hydrogen results in a dramatic decrease in predicted HL60 activity, while LDON remains almost unchanged. This observation is correlated with the observed differences between the two models in region A (see above). The dramatically lower cytotoxicity of example **2a** in comparison with **2b** is thus explained by the model through the lack of the C-3 OH, while the influence of the OH at C-3′ in the benzofuran moiety appears to be insignificant. Analogous predictions were made for the corresponding 3- and 3′-deoxy derivatives of the potent antileishmanial compounds, **2h**, **2i** and **2g**. Consistent with the above mentioned results, in each case the 3-deoxy analogue was estimated to be considerably less cytotoxic than the parent compound while the LDON activity was predicted to be only slightly lower; predicted data for the derivatives of **2g** (**p3**–**p5**) are reported in Table 4. It can thus be expected that deoxygenation at C-3 will not influence LDON activity to the same extent as HL60 toxicity, so that a somewhat higher degree of selectivity might possibly be found in these compounds.

Secondly, the influence of the alkyl side chains was investigated by systematic replacement of the methyl ester groups at C-9 and C-9′ of **p2** with esters of higher alcohols of variable size and branching (as examples, predictions for the *n*-butyl derivatives **p20** and **p21** in comparison with **p2** are given in Table 4; a full table of all probe compounds' structures and predicted binding energies is available as supplementary material). Exchange of the methyl ester at C-9 by more bulky and lipophilic alkyl moieties (ethyl, *n*- and *i*-propyl, *n*-, *i*- and *tert*-butyl) was predicted to result in a dramatic decrease of cytotoxicity (typically, the calculated binding energy was less favourable by $\approx 1\,\mathrm{kcal\,mol^{-1}}$; compare **p21** with **p2**). Analogous replacement of the C-9′ methyl ester by the mentioned alkyl groups in most cases led to a less pronounced decrease of predicted cytotoxicity; in case of the *n*-butyl derivative **p20**, even a slight increase was observed. Contrastingly, replacement at both positions resulted in similarly high impact on antileishmanial activity, which was consistently predicted to increase with the size of the ester group.

It may thus be expected that the hydrophobic receptor subsite interacting with the C-9 ester group (region C in Fig. 2) is more sterically restricted in case of the HL60 binding site than in the LDON receptor so that in conclusion increased steric bulk of the C-9 substituent appears the major factor responsible for the comparatively low cytotoxicity of example **2h**, **2i** and **2g**. Their high antileishmanial activity in comparison with example **2b** is explained by their higher lipophilicity and improved van der Waals interactions with the LDON binding site. The selectivity of such ester derivatives towards *L. donovani* according to our results should moreover be preserved or even further increased by eliminating the C-3 OH group. Since such 3-deoxy analogues can be expected to show higher stability in comparison with the 3,4-diphenols with respect to oxidative degradation, it appears well justified to test them in the future.

3. Material and methods

3.1. Chemistry

Synthesis of **2a**–**d**, **3a**–**d**, **4a**–**e**, **5d** and **6d** has been published before.[6,10] Compound **4d** and **4e** correspond to the naturally occurring lignans 3′,4-di-*O*-methylcedrusin and 4-*O*-methylcedrusin, respectively.[11] Synthesis of the dihydrobenzofuran derivatives **2f**–**i** by oxidative dimerisation of the caffeic acid esters **1f**–**I** as described before for caffeic acid methyl ester, is shown in Scheme 1.[6] Synthesis of the benzofuran derivatives **5**–**10j** starting from the protected dihydrobenzofuran derivative **2j**, prepared by acetylation of **2c**, and of the benzofuran derivatives **5**–**7d**, starting from the dihydrobenzofuran **2d**, is shown in Scheme 2. All benzofurans are formed by dehydrogenation of dihydrobenzofurans. Free phenolic groups are protected by acetylation using acetic anhydride in pyridine catalysed by *N*,*N*-dimethylaminopyridine (DMAP). This is not necessary in the fully methylated **2d**. Compounds **2d** and **2j** can be dehydrogenated to **5d** and **5j**, respectively, using 2,3-dichloro-5,6-dicyano-1,4-benzoquinone (DDQ). Catalytic hydrogenation of **5d** and **5j** yielded **6d** and **6j**, respectively, both with a saturated side chain; further reduction of the methyl ester functionalities with $LiAlH_4$ in tetrahydrofurane (THF) yielded the primary alcohols **7d** and **7j**. During reduction of **6j** with $LiAlH_4$, the protecting acetyl group is lost,

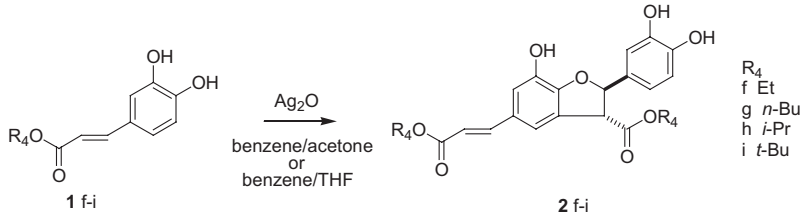

Scheme 1.

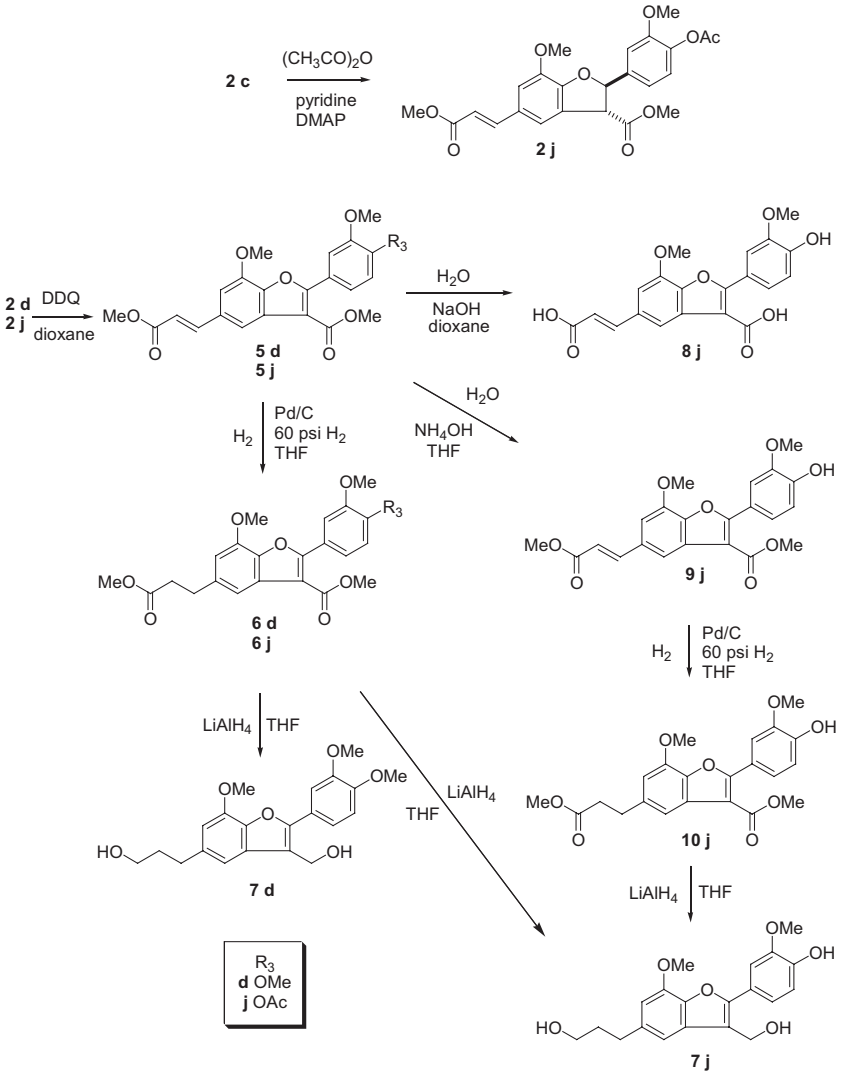

Scheme 2.

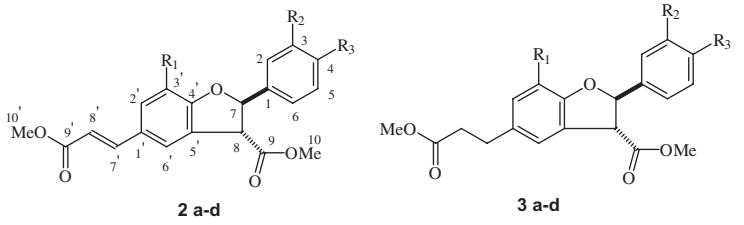

2 a-d

3 a-d

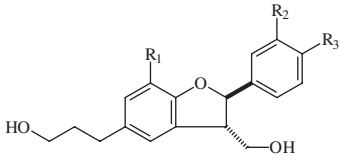

4 a-e

	R_1	R_2	R_3
a	H	H	OH
b	OH	OH	OH
c	OMe	OMe	OH
d	OMe	OMe	OMe
e	OH	OMe	OMe

leading to **7j**. Alternatively, hydrolysis of **5j** with NaOH resulted in the deacetylated **8j**, with two carboxylic acid functionalities. During mild hydrolysis of **5j** with ammonia only the acetyl group is removed (**9j**). In the same way as for **5j**, compound **9j** can be reduced to **10j** and finally to **7j**. All compounds were racemic mixtures with a *trans* configuration in the dihydrobenzofuran ring, and were characterised by ^{1}H and ^{13}C NMR, MS, high resolution MS, elemental analysis (C, H), and/or HPLC as described before.[6,10]

3.2. Cytotoxicity and antiprotozoal activity

Evaluation of test compounds in an in vitro human disease oriented tumour cell line screening panel, consisting of 60 human tumour cell lines, at the National Cancer Institute (NCI, Bethesda, MD, USA) has been published before.[6]

Evaluation against the protozoa *L. donovani* (axenic amastigotes), chloroquine resistant *P. falciparum* (strain K1), *T.b. rhodesiense* and *T. cruzi*, and for cytotoxicity on L6 cells was performed according to experimental procedures described before.[12]

3.2.1. Leishmania macrophage assay. Mouse peritoneal macrophages were seeded in RPMI 1640 medium with 10% fetal bovine serum into Lab-tek 16-chamber slides. After 24 h *L. donovani* amastigotes were added at a ratio of 3:1 (amastigotes to macrophages). Next day the medium was replaced by fresh medium containing different drug concentrations and incubated at 37 °C for 96 h. Then the medium was removed, the slides fixed with methanol and stained with Giemsa. The ratio of infected to non-infected macrophages was determined microscopically, and expressed as percentage of the control and the IC_{50} value calculated by linear regression.

3.3. QSAR

3.3.1. Biological data. The calculations were carried out on the basis of IC_{50} data for cytotoxicity against the HL60 cell line (see Supporting information) and growth inhibition against axenic amastigotes of *L. donovani*. The IC_{50} values were transformed to molar concentrations and converted to binding energies (ΔG^{0}_{293} (kcal mol^{-1}) $= 10^{-3} - RT \ln 1/IC_{50}$ (M), $T = 293\,K$) to be used for the *Quasar* calculations. In cases where only cutoff values for the biological data existed (IC_{50} > cutoff value), an arbitrary value of 100 μM was used.

3.3.2. Molecular modelling. Molecular models of all compounds were generated using Hyperchem v. 7. Each compound was modelled by applying the appropriate changes to an initial low-energy conformer of **2a**, which was used as template. All models were energy minimised to an RMS gradient <0.05 kcal mol^{-1} Å^{-1} in the MM+ force field. The resulting geometries were minimised using the AM1 hamiltonian to an RMS gradient <0.05 kcal mol^{-1} Å^{-1}. Atomic partial charges were derived from the AM1 wavefunctions. The molecular models were superposed with respect to the benzofuran benzene ring. Models were stored in Tripos mol2 format and used as input for Quasar.

Training and test set subdivision (Table 3) was performed on the basis of maximally diverse subset calculation based on typed atom triangle fingerprints (MOE).[13] In case of the cytotoxicity data, 23 compounds were included in the modelling process. Eighteen compounds showing maximum structural diversity were used as the training set, the five remaining compounds were used as the test set. In the antileishmanial data set ($n = 20$), 15 compounds constituted the training set, while five compounds were used for external predictions.

3.3.3. *Quasar* receptor surface modelling.[8,9] *Quasar* v. 4.0 for Windows was used. For each compound, one single conformer was taken into account (inclusion of up to five further low-energy geometries obtained by a stochastic conformational search[13] did not lead to improvement of the presented models). All six possible induced fit modes were evaluated. The model population submitted to the genetic algorithm of *Quasar* in each case consisted of 200 individual models so that the presented models represent the average of 200 individual offspring models. Internal predictivity was assessed by leave 1/3 out cross-validation. Termination criteria for the model evolution were (1) $q^2 \geqslant 0.900$, (2) RMS error of internal predictions $\leqslant 0.236$, (3) 5000 cross-over steps. A variety of different settings with respect to the incorporation of polarisation effects, weighting of solvation energy and entropy contributions as well as diffusion of particle properties were evaluated. The presented models represent the optimum settings found with respect to external predictivity (squared correlation coefficient of experimental versus predicted ΔG^{0} values for the test set, p^2). For both data sets the validity of the models was confirmed by randomly assigning the biological data to the compounds and repeating the simulations under otherwise identical conditions (scramble tests). The average p^2 of three scramble tests was −0.69 for HL60 and −1.04 for LDON, proving the sensitivity of the models to the biological data for which they were to establish quantitative structure–activity relationships. For both data sets, the optimum correlations were obtained when both, polarisation effects (Lig-Rec and Rec-Lig) as well as diffusion of particle properties were applied (both with their default settings). Predictions for non-existent compounds (**p1**–**p26**; Table 4 and Supporting information) were made following essentially the same protocol as described above. A full list of *Quasar* output can be obtained in electronic form on request from Schmidt (schmidtt@uni-duesseldorf.de).

Acknowledgements

This work was financially supported as a Concerted Action by the Special Fund for Research of the University of Antwerp. The National Cancer Institute (NCI, Bethesda, MD, USA) is kindly acknowledged for evaluation of our compounds in their human tumour cell line screening panel. This investigation received financial support from the UNDP/World Bank/WHO Special

Programme for Research and Training in Tropical Diseases (TDR).

Supplementary data

Supplementary data associated with this article can be found, in the online version, at doi:10.1016/j.bmc.2004.10.058.

References and notes

1. Davis, A. J.; Murray, H. W.; Handman, E. *Trends Parasitol.* **2004**, *20*, 73.
2. Werbovetz, K. A. *Mini Rev. Med. Chem.* **2002**, *2*, 519.
3. Jayanarayan, K. G.; Dey, C. S. *J. Clin. Pharm. Ther.* **2002**, *27*, 313.
4. Del Rey, B.; Ramos, A. C.; Caballero, E.; Inchaustti, A.; Yaluff, G.; Medarde, M.; Rojas de Arias, A.; San Feliciano, A. *Bioorg. Med. Chem. Lett.* **1999**, *9*, 2711.
5. Barata, L. E. S.; Santos, L. S.; Ferri, P. H.; Phillipson, J. D.; Paine, A.; Croft, S. L. *Phytochemistry* **2000**, 589.
6. Pieters, L.; Van Dyck, S.; Gao, M.; Bai, R.; Hamel, E.; Vlietinck, A.; Lemière, G. *J. Med. Chem.* **1999**, *26*, 5475.
7. Apers, S.; Vlietinck, A.; Pieters, L. *Phytochem. Rev.* **2003**, *2*, 201–217.
8. Vedani, A.; Dobler, M. *J. Med. Chem.* **2002**, *45*, 2139.
9. Quasar manual: Biographics Laboratory 3R, Basel, Switzerland; http://www.biograf.ch.
10. Van Dyck, S. M. O.; Lemière, G. L. F.; Jonckers, T. H. M.; Dommisse, R. *Molecules* **2000**, *5*, 153.
11. Pieters, L.; Calomme, M.; De Bruyne, T.; Claeys, M.; Vanden Berghe, D.; Vlietinck, A. *J. Nat. Prod.* **1993**, *56*, 899.
12. Mbwambo, Z. H.; Apers, S.; Moshi, M. J.; Kapingu, M. C.; Van Miert, S.; Brun, R.; Cos, P.; Pieters, L.; Vlietinck, A. *Planta Med.* **2004**, *70*, 706–710.
13. The molecular operations environment, Chemical Computing Group, Montreal, Canada; http://www.chemcomp.com.